Supporting Information

Enhancing the cycling stability of MgH_2 by nitrogen modified titanate

*Ren Zou[a,b‡], Jialing Li[a,b‡], Weijin Zhang[a], Gangtie Lei[b], Zhi Li,[c] Hujun Cao[a,d]**

a) Dalian Institute of Chemical Physics, Chinese Academy of Sciences, Dalian, 116023, China

b) Key Laboratory of Environmentally Friendly Chemistry and Applications of Ministry of Education, School of Chemistry, Xiangtan University, Hunan, 411105, China

c) National Engineering Research Center of Coal Gasification and Coal-Based Advanced Materials, Shandong Energy Group Co. LTD. Jinan, 250000, China

d) Center of Materials Science and Optoelectronics Engineering, University of Chinese Academy of Sciences, Beijing, 100049, China.

E-mail: caohujun@dicp.ac.cn

Experimental section

1.1 Samples preparation

MgH_2 (99%), and anatase TiO_2 (99.8% metal basis 25 nm particle size) powders were commercially purchased from Alfa-Aesar, and Macklin respectively. The powders were used without further treatment. High purity potassium amide obtained by ball milling of potassium metal (after remmoving the mineral oil by washing 3 time in cyclohexane, Aladdin, 95%) in an ammonia atmosphere.[1] All samples were prepared in a glovebox with an argon circulative purification system (O_2 < 0.1 ppm, H_2O < 0.1 ppm) to avoid the contamination of oxygen and moisture. Potassium amide reduced TiO_2 catalyst (named N-KTiO) was prepared by independently ball milling KNH_2 and TiO_2 at mass ratio of 0.33 to 1 for 3 h (precursor), and then annealing at 450 ℃ for 5 h. After that, a preselected amount of each catalyst obtained was added into pure MgH_2 powder and ball-milled (named + *x* N-KTiO, where mass quantity "*x*" equals 0, 2.5, 5, 10 wt.%). Ball milling of all the MgH_2 composites lasted for 10 h with batch weight of 2 g. All the milling processes were performed using a Retsch PM 400 mill at room temperature with a rotation speed of 200 RPM. The mixtures were sealed in 150 ml stainless steel vials in a glovebox with a ball-to-powder weight ratio (BPR) of about 100:1. The milling process was interrupted for 30 s after every 3 min of rotation to dissipate accumulated heat.

1.2 Sample characterizations

Powder X-ray diffraction (XRD) measurements were conducted using an X'Pert3 Materials Research Diffractometer (Malvern Panalytical) with Cu Kα radiation (λ = 0.154 nm) at 40 kV and 40 mA. Samples were loaded into steel sample holders and covered with Kapton film to avoid contamination during the measurements. Each measurement was done at a scan speed of 10°/min over diffraction angles of 5 to 90°. The microstructure and morphology of the samples were investigated using JSM-7800F scanning electron microscopy (SEM) equipped with an energy-dispersive X-ray spectroscopy (EDS) analysis unit, and JEM-2100 transmission electron microscopy (TEM). For TEM analysis, the samples were dispersed onto a thin holey carbon film in the glovebox to avoid the influence of oxygen and moisture. Image processing was performed using Digital Micrograph (Gatan) software. X-ray photoelectron spectroscopy (XPS, Thermo Fisher Scientific, ESCALAB 250Xi, Al-Kα = 1486.6 eV) technique was used to analyse the surface state of samples under different states. The binding

energy was calibrated using C−C binding energy at 284.8 eV as a reference. FT-IR were conducted on a Tensor II FTIR spectrometer in a diffuse reflection mode.

Thermal decomposition properties of the samples were first investigated by a homemade temperature-programmed desorption system equipped with a mass spectrometer (HPR20, Hiden) (TPD-MS). About 15-20 mg of the samples were loaded into an air-tight sample holder and sealed to the reactor in the glovebox. The analysis was carried out between room temperature and 400 °C at a heating rate of 2 °C/min under 20 mL/min argon flow. Volumetric desorption and absorption measurements of the samples were carried out using a commercialized sievert's apparatus (HPSA-auto device, China), in which the modified Benedict-Webb-Rubin (MBWR) EOS was used to calculate the hydrogen storage capacity. For desorption, the samples were heated up from room temperature to 400 °C, with a heating rate of 2 °C/min under 0.001 bar while the re-absorption process was conducted at room temperature under 1, 10, 30, 50, bars of H_2 backpressure. The cyclic capacity of the sample was tested at 300 °C under 0.3 and 30 bars of H_2 for de/re-absorption. The thermodynamic properties of the samples were evaluated by using a conventional Hy-Energy PCT pro-2000 pressure-composition-isotherm (PCI) analyser. PCI re/de-sorption evaluation was conducted at 310, 320, 330, while the thermodynamic information was derived from a PCT plot using Van't Hoff equation. This plot is a function of the logarithm of equilibrium pressure with the inverse of temperature.[2]

$$ln^{PH_2} = \frac{\Delta H}{RT} - \frac{\Delta S}{R}$$

Where PH_2, ΔH, and ΔS are the hydrogen equilibrium pressure, enthalpy, and entropy change, respectively.

The apparent activation energy E_a of each sample under investigation was determined by using the Kissinger method, through obtaining the peak maximum in TPD-MS measurements. Samples were heated from room temperature to 400 °C with heating rates of 2, 4, 6, and 8 °C/min under 20 mL/min of argon flow. The Ea was calculated using the following equation:[3]

$$ln^{\frac{\beta}{T_p^2}} = \frac{-E_a}{RT_p} + \mathrm{A}$$

Where β is the heating rate, T2 pis the peak temperature of desorption given by the result of TPD-MS, R is the gas constant, A is a pre-exponential factor, and E_a is the activation energy obtained from the slope.

To determine the optical band gap, a UV-visible diffuse reflectance (Jasco V-750 UV-visible spectrophotometer) was used. The Kubelka–Munk equation:[4]

$$F(R) = \frac{(1-R)^2}{2R} = \frac{\alpha}{s}$$

where R: relative reflectance; α: absorption coefficient; s: scattering coefficient), was used to determine the optical absorbance for each material. The optical reflectance curves were taken to form a Tauc plot of $F(R)$hν against photon energy by using the Tauc equation:[5]

$$[F(R)h\nu]^n = B(Eg - h\nu)$$

where B is a constant. A sample with a direct band gap shows a linear dependence if n=2, whereas indirect gaps have a linear dependence if n=1⁄2. The optical band gaps were obtained from the extrapolation of the linear part of the curve.

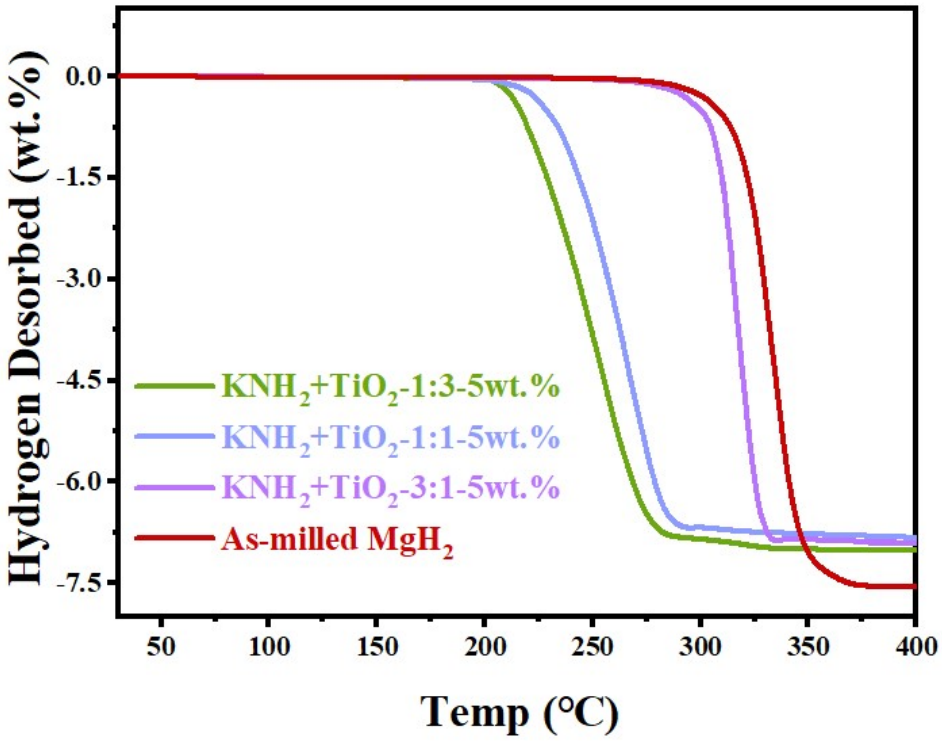

Figure S1. Volumetric dehydrogenation curves of MgH_2 with 5 wt% of KNH_2 doped TiO_2 at mass ratios of 1, 3, and 9 to 3.

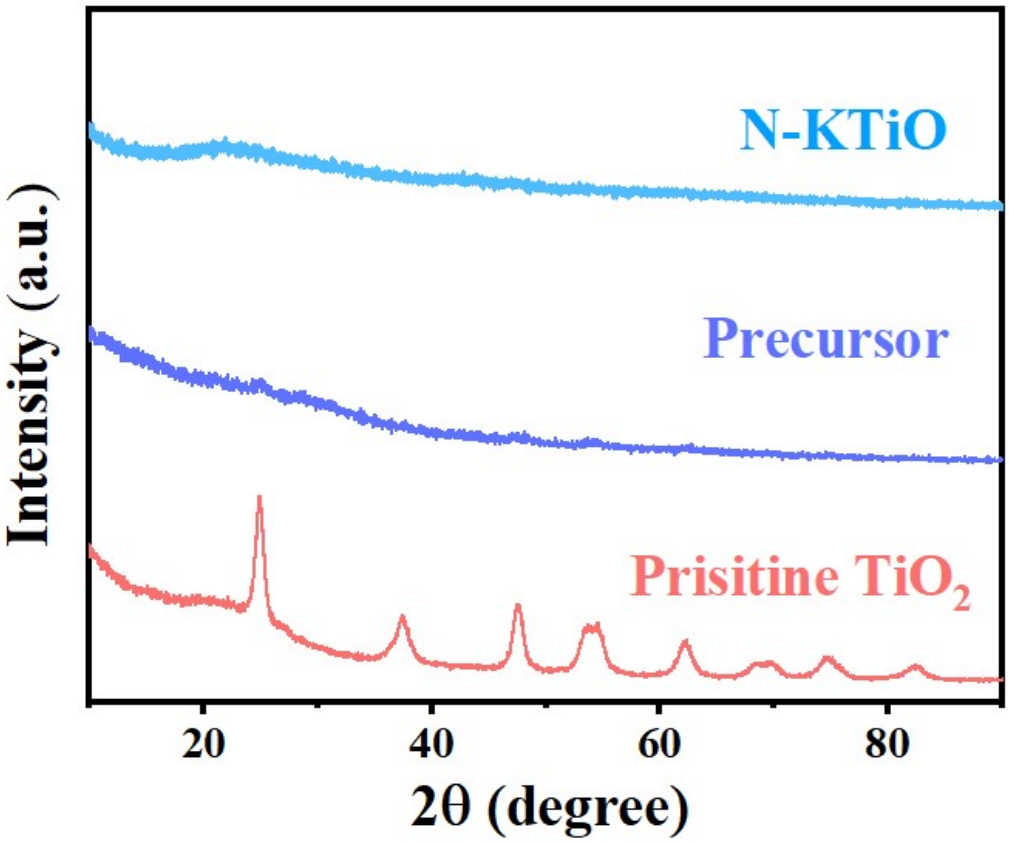

Figure S2. XRD patterns of the pristine TiO_2, precursor and N-KTiO.

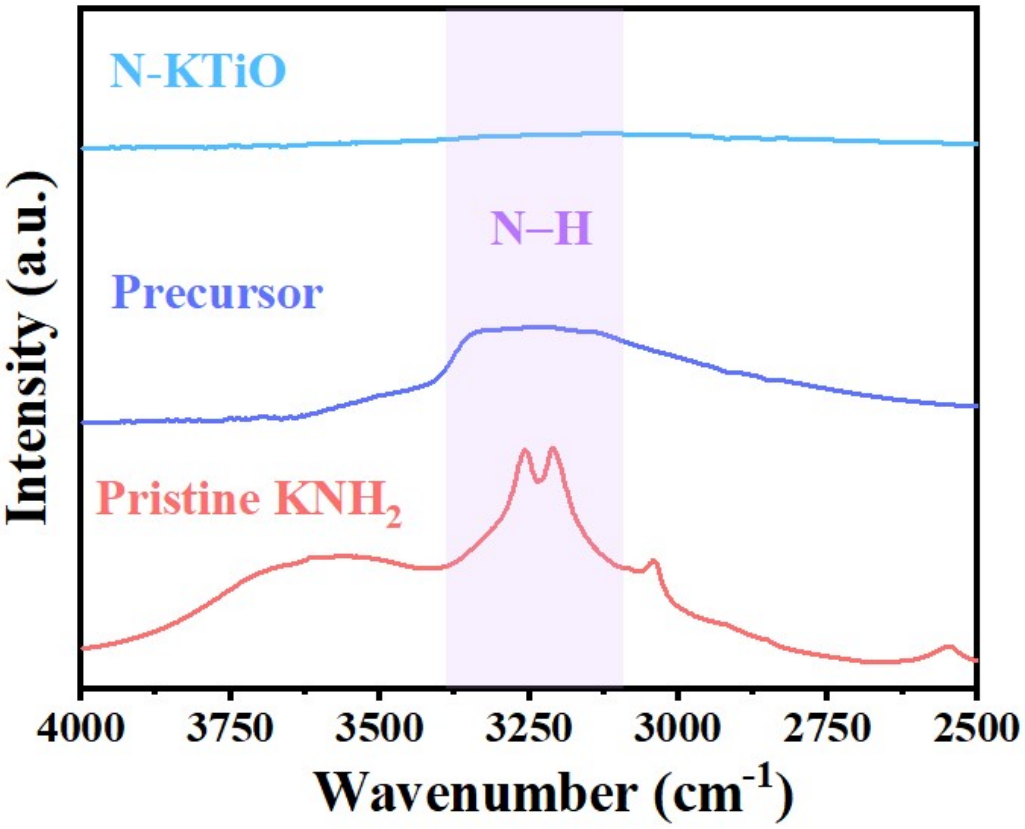

Figure S3. FT-IR spectra of the pristine KNH_2, precursor and N-KTiO.

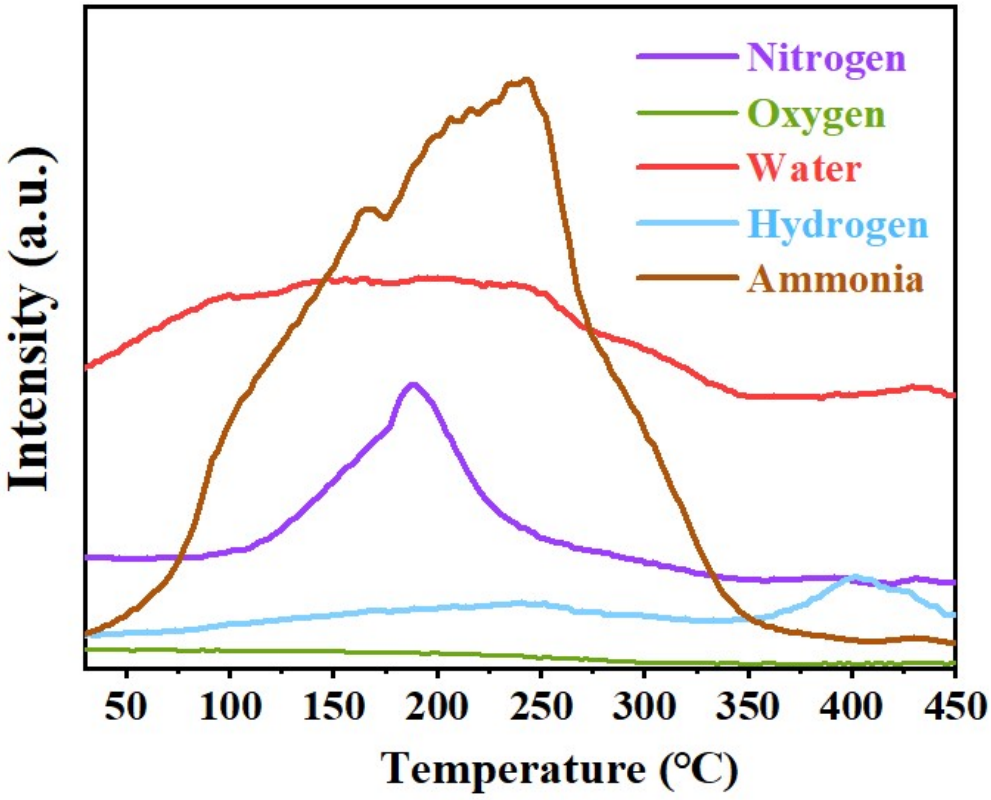

Figure S4. TPD-MS curve of the precursor.

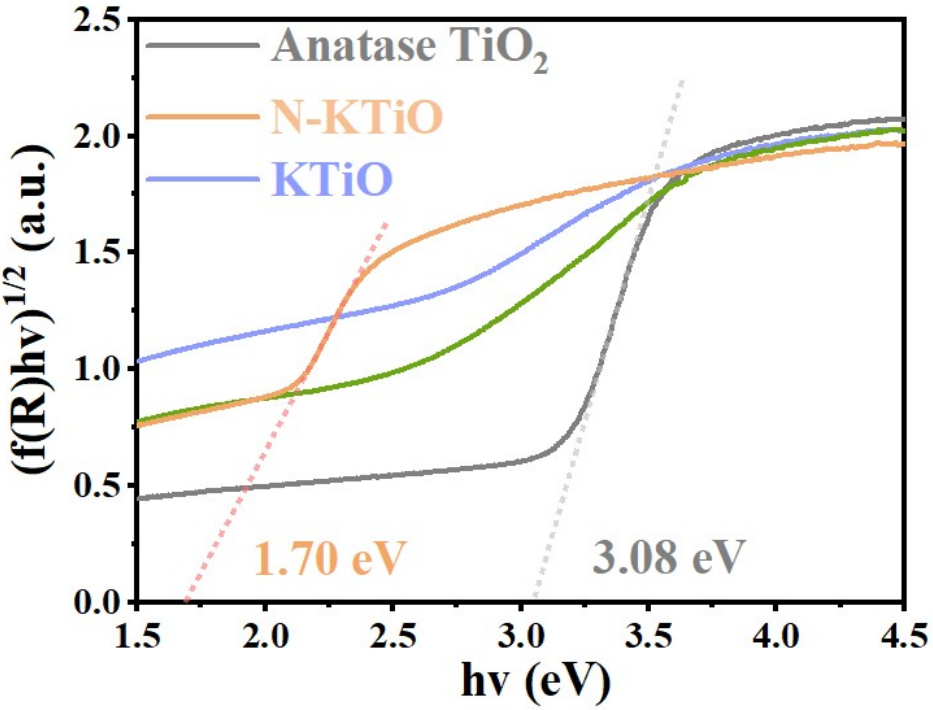

Figure S5. Tauc plots for different samples (indirect gaps, n=2).

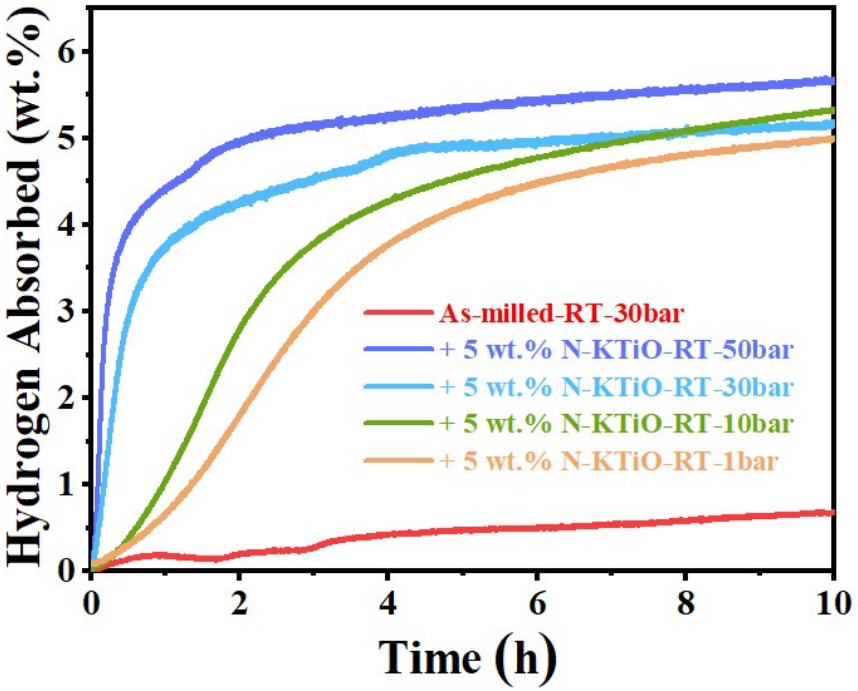

Figure S6. Room-temperature hydrogen absorption curves of the + 5 wt.% N-KTiO sample at 1, 10, 30, and 50 bars of hydrogen pressures.

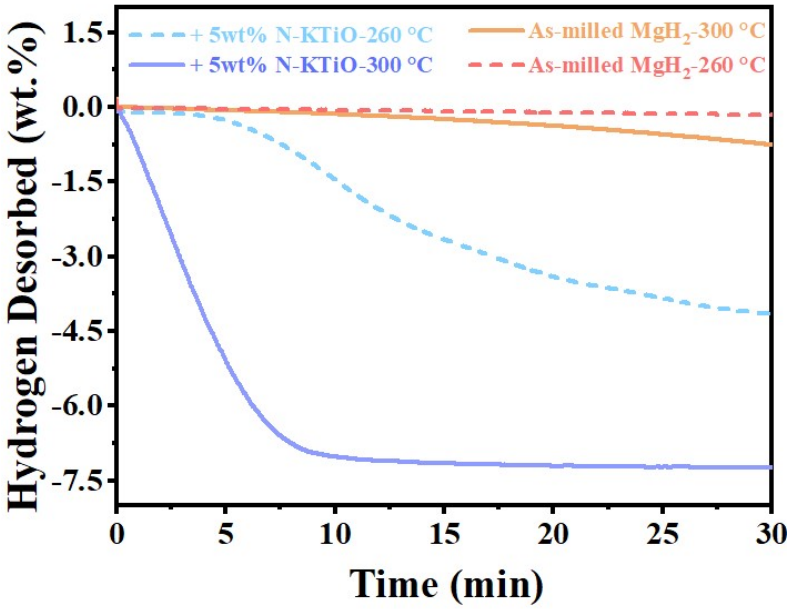

Figure S7. Isothermal dehydrogenation at 260 and 300 °C for the as-milled MgH_2 and + 5 wt.% N-KTiO sample.

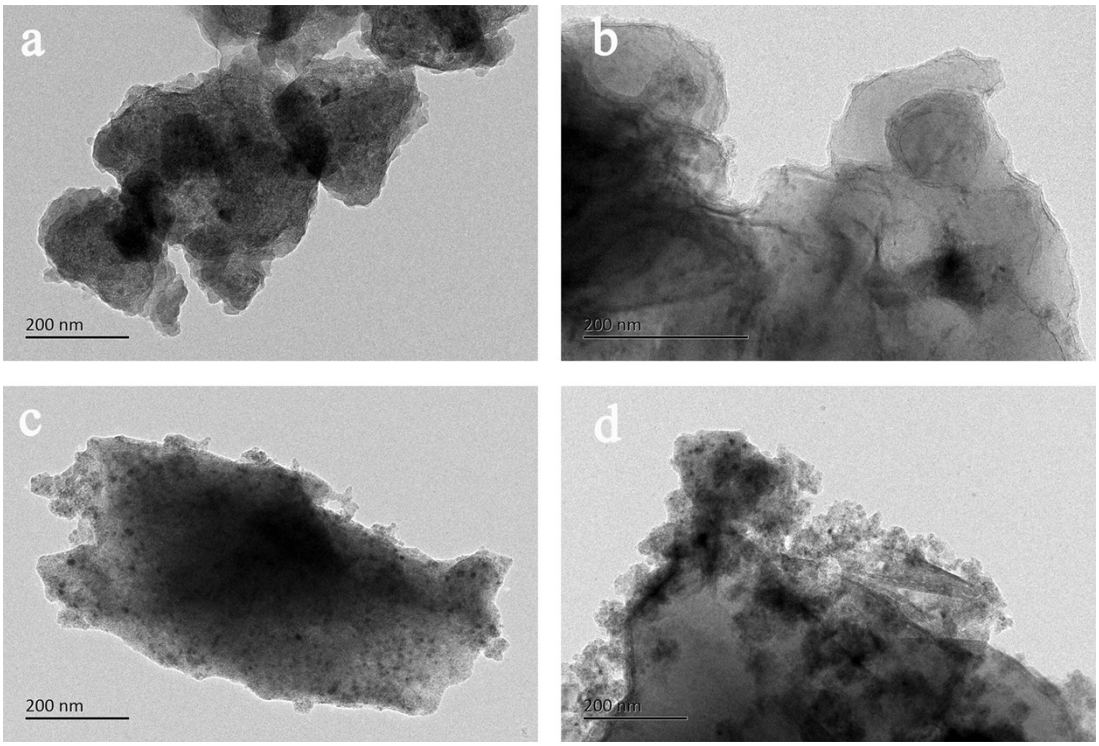

Figure S8. TEM images of (a) the as-milled, (b) the 1st dehydrogenated, (c) the 200th hydrogenated, and (d) the 200th dehydrogenated samples.

References:

1. J. Wang, G. Lei, T. He, H. Cao and P. Chen, *Journal of Energy Chemistry*, 2022, **69**, 555-560.
2. M. Paskevicius, D. A. Sheppard and C. E. Buckley, *Journal of the American Chemical Society*, 2010, **132**, 5077-5083.
3. H. E. Kissinger, *Analytical chemistry*, 1957, **29**, 1702-1706.
4. A. P. Finlayson, V. N. Tsaneva, L. Lyons, M. Clark and B. A. Glowacki, *physica status solidi (a)*, 2006, **203**, 327-335.
5. J. Tauc, R. Grigorovici and A. Vancu, *physica status solidi (b)*, 1966, **15**, 627-637.